Human Mitochondrial DNA Polymerase Holoenzyme: Reconstitution and Characterization†

Allison A. Johnson, Yu-chih Tsai, Steven W. Graves, and Kenneth A. Johnson*

Institute for Cellular and Molecular Biology, A4800, MBB 3.122, University of Texas at Austin, Austin, Texas 78712

Received September 8, 1999; Revised Manuscript Received October 29, 1999

ABSTRACT: We have reconstituted the holoenzyme of the human mitochondrial DNA polymerase from cloned and overexpressed catalytic and accessory subunits. We have examined the polymerization activity of the catalytic subunit alone and of the holoenzyme to establish the function of the accessory subunit in this two subunit enzyme. The accessory subunit associates with the catalytic subunit with a dissociation constant of 35 ± 16 nM as measured by the concentration dependence of its effect in stimulating maximal DNA binding and polymerization. At saturating concentrations, the accessory subunit contributes to every kinetic parameter examined to facilitate tighter binding of DNA and nucleotide and faster replication. The accessory protein makes the DNA binding 3.5-fold tighter (K_d of 9.9 ± 2.1 nM compared to 39 ± 10 nM for the catalytic subunit alone) without significantly affecting the DNA dissociation rate (0.02 ± 0.001 compared to 0.03 ± 0.001 s^{-1}). The ground-state nucleotide binding is improved from 4.7 ± 2.0 to 0.78 ± 0.065 μM, and the maximum DNA polymerization rate is increased from 8.7 ± 1.1 to 45 ± 1 s^{-1} by the addition of the accessory protein. This leads to an increase in processivity from an estimated 290 ± 46 to 2250 ± 162. Although the accessory protein has been described as a "processivity factor" because of its effect on the ratio of rate constants defining processivity, this terminology falls short of adequately describing the profound effects of the small subunit on nucleotide-binding and incorporation catalyzed by the large subunit. By using the complete holoenzyme, we can now proceed with a comprehensive analysis of the structural and mechanistic determinants of enzyme specificity that govern toxicity of nucleoside analogues used in the treatment of viral infections such as AIDS.

Replication of mitochondrial DNA is catalyzed by the mitochondrial DNA polymerase, DNA polymerase γ. Mutation of mitochondrial DNA, which encodes several proteins required for respiration, leads to loss of mitochondrial function (*1*). Mutations and deletions in mitochondrial DNA are linked to degenerative diseases including Kearns-Sayre syndrome and ragged-red fiber disease (*2*). Additionally, incorporation of antiviral nucleoside analogues into the mitochondrial genome by DNA polymerase γ results in loss of mitochondrial function and causes adverse side effects observed in the treatment of AIDS and Hepatitis B (*3*, *4*). Examining the mechanism of replication by DNA polymerase γ is important to understanding mitochondrial dysfunction arising from errors in polymerization and provides the necessary groundwork to finding nucleoside analogues exhibiting reduced toxicity. Most importantly, formation of a recombinant human mitochondrial DNA polymerase holoenzyme can provide the large amounts of enzyme required for structure−function studies examining nucleoside analogues. These studies may provide quantitative, mechanistic information useful for the design and screening of new antiviral nucleoside analogues that are clinically effective against HIV and exhibit lower toxicity.

DNA polymerase γ isolated from various sources is a two-subunit enzyme consisting of a larger catalytic subunit providing both polymerase and 3′−5′exonuclease activities (*5*−*8*) and a smaller accessory subunit that is thought to act as a "processivity factor" (*9*, *10*). Human DNA polymerase γ is composed of a catalytic subunit of 140 kDa and an accessory subunit estimated to be approximately 54 kDa (*11*). The mitochondrial DNA polymerase has been purified in native form from many organisms (*5*, *6*, *11*, *12*), but low enzyme yield and variable activity has precluded rigorous kinetic characterization. The human catalytic subunit has been cloned (*13*, *14*) and recombinant expression of the catalytic subunit has been accomplished in *Drosophila melanogaster* (*15*) and *Homo sapiens* (*8*, *16*). To date, recombinant expression of the accessory subunit has only been achieved in *Xenopus laevis* (*10*). The cDNA encoding the human accessory subunit has been identified (*9*), but we determined that errors in the sequence precluded our attempts at expression of soluble, active protein. We have now corrected those errors and have succeeded in assembling a complete human mitochondrial DNA polymerase holoenzyme from recombinant large (catalytic) and small (accessory) subunits. We present here our initial assessment of the function of the accessory subunit.

EXPERIMENTAL PROCEDURES

Creation and Expression of Bacterial Construct. A cDNA encoding the accessory subunit of human mitochondrial DNA polymerase was identified through amino acid sequence homology to the *Drosophila* accessory subunit (*9*). The clone was obtained from the I. M. A. G. E. Consortium (Clone ID Number 44673) and was sequenced on both strands. PCR was used to engineer an *Nhe*1 site following the 56th amino

* To whom correspondence should be addressed.Telephone: (512) 471-0434. Fax: (512) 471-0435. E-mail: kajohnson@mail.utexas.edu.

† This work is supported by National Institutes of Health Grant GM44613 (to Kenneth A. Johnson).

10.1021/bi992104w CCC: $19.00
Published on Web 01/27/2000

acid and a *Sal*1 site replacing the stop codon of the open reading frame. The resulting 1287 basepair DNA was restriction digested, purified by agarose gel electrophoresis, and ligated into pET24a (Novagen, Madison, WI). The final open reading frame contained an additional 15 amino acids on the carboxyl terminal end including six histidines to aid in purification (VDKLAAAELHHHHHH). The plasmid was transformed into BL21(DE3) cells. Bacteria were grown to an OD_{600} of 0.5 at 37 °C in Luria Broth containing 50 μg/mL of kanamycin. Expression of the protein was induced by the addition of isopropyl β-D-thiogalactopyranoside to 0.4 mM. After 18 h of induction at 20 °C, cells were collected by centrifugation at 3500 rpm in a Sorvall SLA 3000 rotor at 4 °C.

Preparation of Bacterial Lysate. All procedures were performed at 4 °C. Bacterial cell pellets, typically 16 g from 3 L of bacterial culture, were resuspended in 1/10 of the culture volume in buffer containing 20 mM Tris-HCl, pH 8.0, 500 mM NaCl, 5 mM imidazole, and 0.1% Triton X-100. This mixture was sonicated until it lost viscosity and then it was clarified by centrifugation for 30 min at 40 000 rpm in a Beckman 45Ti rotor. The supernatant was retained for chelating sepharose chromatography.

Chelating Sepharose Chromatography. Chelating sepharose (Amersham Pharmacia Biotech, Piscataway, NJ) was prepared by washing 10 mL of resin with five volumes of distilled water, five volumes of 50 mM $NiSO_4$, and three volumes of binding buffer (20 mM Tris-HCl, pH 8.0, 500 mM NaCl, 5 mM imidazole). The clarified supernatant of the bacterial lysate was stirred with preequilibrated resin for 30 min. The mixture was centrifuged for 10 min in a Sorvall SLA-3000 at 3500 rpm to collect the resin. The resin was resuspended with 50 mL of wash buffer (20 mM Tris-HCl, pH 8.0, 500 mM NaCl, 100 mM imidazole), recentrifuged, resuspended in 20 mL of wash buffer, and poured into a 10 cm length by 1 cm diameter column. The column was washed with ten column volumes of wash buffer. Protein was eluted from the column with three column volumes of elution buffer (20 mM Tris-HCl, pH 8.0, 500 mM NaCl, 370 mM imidazole). Fractions containing the accessory subunit, as analyzed by SDS-PAGE, were collected and dialyzed into buffer containing 50 mM Tris-HCl, pH 7.2, 50 mM NaCl, 5 mM EDTA, and 10% glycerol.

Mono-S Chromatography. Dialyzed protein was loaded at 0.5 mL/min onto a preequilibrated HR10/10 Mono-S column (Amersham Pharmacia Biotech, Piscataway, NJ). The column was washed with three column volumes of buffer and the protein was eluted over five column volumes by a salt gradient with buffer containing 50 mM Tris-HCl, pH 7.2, 1 M NaCl, 5 mM EDTA, and 10% glycerol. Fractions were analyzed by SDS-PAGE and those containing the accessory subunit were pooled and dialyzed into 50 mM Tris-HCl, pH 8.4, 100 mM NaCl, 1 mM DTT, 5 mM EDTA, 50% glycerol. The dialysate was divided into 5 μL aliquots, frozen in liquid nitrogen, and stored at −80 °C. Protein concentration was determined by A_{280}, using an extinction coefficient of 71894 AU/M/cm (*17*).

Western Blot. Samples were separated by SDS-PAGE and blotted to nitrocellulose. Blots were incubated with a 1:5000 dilution of anti-6X histidine (Invitrogen, Carlsbad, CA) followed by a 1:2000 dilution of antimouse secondary antibody conjugated to alkaline phosphatase.

Purification of the Catalytic Subunit. Purification of the protein from a baculovirus expression system (Life Technologies, Gaithersburg, MD) was performed as described in ref *8*. Nominal protein concentrations were determined by absorbance measurements.

Preparation of Substrate DNA. The primer sequence was 5′-GCCTCGCAGCCGTCCAACCAACTCA-3′, and the template sequence was 5′-GGACGGCATTGGATCGAGGTTGAGTTGGTTGGACGGCTGCGAGGC-3′ (*18*). Primer was 5′ ^{32}P-labeled with T4 polynucleotide kinase according to the manufacturer's instructions (Life Technologies, Gaithersburg, MD). The reaction was terminated by incubation at 95 °C for 5 min, and the unincorporated nucleotide was removed using a Bio-Spin 6 column (Biorad, Hercules, CA). Labeled 25-mer primer was combined with 45-mer template at an equi-molar ratio, heated to 95 °C, and cooled to room temperature to allow annealing to occur.

Single-Nucleotide Incorporation DNA Polymerase Assay. The catalytic and accessory subunits of DNA polymerase γ were combined and preequilibrated for 20 min on ice prior to each experiment. DNA, reaction buffer, and water were then added and the mixtures were further incubated for 20 min on ice. For pre-steady-state assays, enzyme−DNA complexes (140 nM catalytic subunit, 500 nM 25/45-mer primer template, 50 mM Tris-HCl, pH 7.5, 100 mM NaCl, ±800 nM accessory subunit) were combined with an equal volume of nucleotide−magnesium mix (500 μM dATP, 5 mM $MgCl_2$, 50 mM Tris-HCl, pH 7.5, 100 mM NaCl) at 37 °C using a RQF-3 Rapid Chemical Quench Flow instrument (KinTek Corporation, Austin, TX). Final reaction solutions contained 70 nM catalytic subunit, ±400 nM accessory subunit, 250 nM 25/45-mer DNA, 250 μM dATP,[1] and 2.5 mM $MgCl_2$. Reactions were quenched with 0.3 M EDTA at various times. The amount of product formed as a function of time was fit to the burst equation ($[26mer] = A[1 - e^{-kt}] + k_{cat}t$). For steady-state assays, experiments were performed by adding equal volumes of enzyme/DNA mix to Mg^{2+}/dATP mix and removing aliquots at various times. Final reaction solutions contained 25 nM catalytic subunit, ±140 nM accessory subunit, 1 μM 25/45-mer DNA, 500 μM dATP, 50 mM Tris-HCl, pH 7.5, 100 mM NaCl, 2.5 mM $MgCl_2$. Reactions were quenched after various times with 50% formamide gel loading buffer containing 0.25 M EDTA. The amount of product formed vs time was fit to a straight line.

Dissociation Constant for Subunit Interaction. A fixed concentration of the catalytic subunit was preequilibrated for 20 min on ice with increasing concentrations of accessory subunit. Enzyme was then equilibrated with DNA for an additional 20 min on ice. After the reaction components were warmed to 37 °C, an equal volume of Mg^{2+}/dATP mix was rapidly added to the enzyme/DNA mix, and the reactions were quenched with 0.3 M EDTA at various times. Final reaction solutions contained 40 nM catalytic subunit, 200 nM 25/45-mer DNA, 50 μM dATP, 50 mM Tris-HCl, pH 7.5, 100 mM NaCl, 2.5 mM $MgCl_2$, and a range of 0 to 400 nM accessory subunit. Product 26/45-mer DNA was quantified, and the data were plotted and fit to the burst equation

[1] Abbreviations: dATP, deoxyadenosine triphosphate; dTTP, deoxythymidine triphosphate; EDTA, (ethylenediamine)-tetraacetic acid; DTT, dithiothreitol; HIV-1, human immunodeficiency virus type 1.

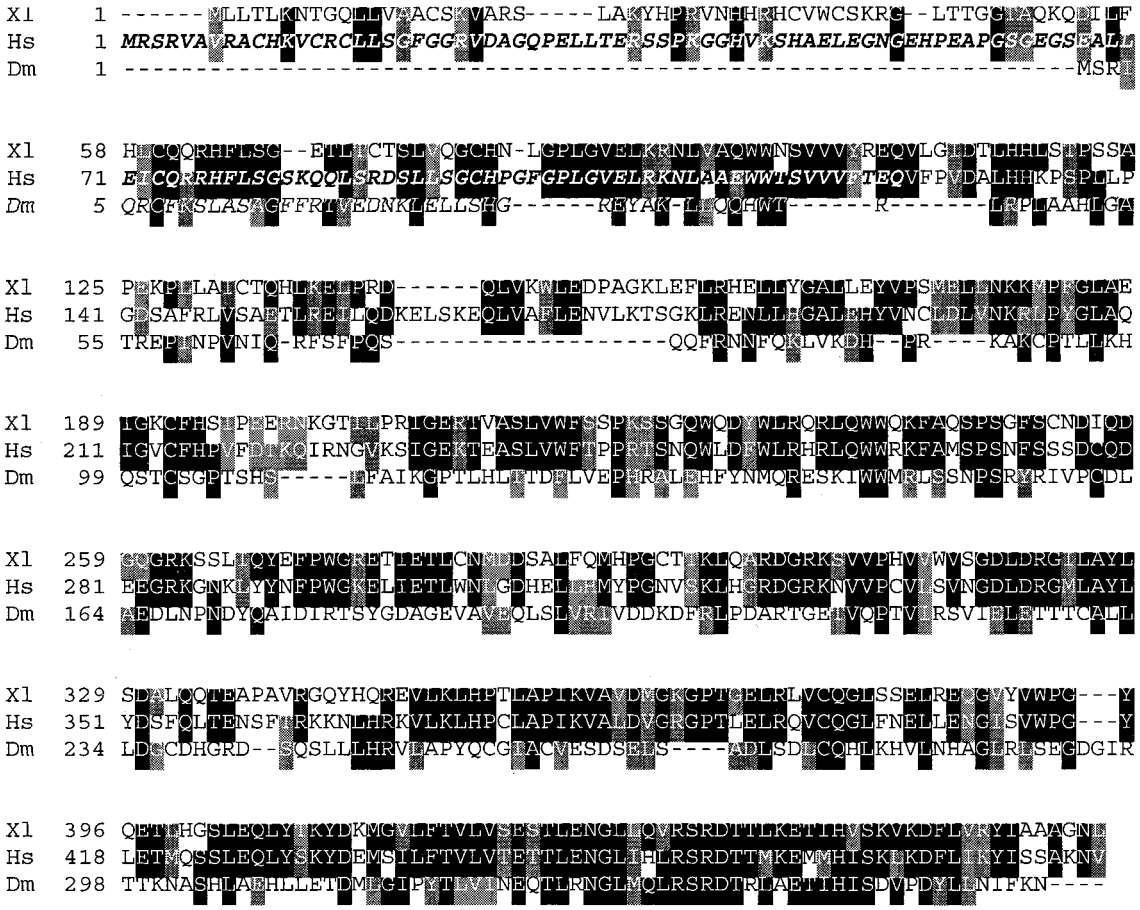

FIGURE 1: Protein sequence alignment of known mitochondrial DNA polymerase accessory subunits. The amino acid sequences of the *Homo sapiens* (Hs), *Xenopus laevis* (Xl), and *Drosophila melanogaster* (Dm) accessory subunits were aligned using Clustal X. The extended sequence of the human protein is shown in bold/italics. Black-shading indicates amino acid identity, while gray-shading indicates similarity of amino acids.

([26mer] = $A[1 - e^{-kt}] + k_{cat}t$) where A represents the burst amplitude. The burst amplitude as a function of accessory subunit concentration was then plotted and fit to the quadratic equation ([E·DNA] = $0.5(K_d + C_t + A_t)^2 - [0.25(K_d + C_t + A_t)^2 - (C_tA_t)]^{1/2}) + B$ where C_t and A_t represent the catalytic and accessory subunit concentrations and B represents the amount of product formed in the absence of the accessory subunit.

Active Site Titration with DNA. A fixed concentration of enzyme was combined with increasing concentrations of DNA 25/45-mer, allowed to equilibrate for 20 min on ice, and then reacted with an equal volume of nucleotide at 37 °C. Reactions were quenched after 1 s by the addition of 0.3 M EDTA. Final reaction conditions were 70 nM catalytic subunit, 400 nM accessory subunit, 250 μM dATP, 50 mM Tris-HCl, pH 7.5, 100 mM NaCl, 2.5 mM $MgCl_2$, and a range of 2.5 nM to 250 nM 25/45-mer DNA. The amount of product 26-mer DNA was plotted as a function of substrate 25/45-mer DNA concentration and the data were fitted to the quadratic equation ([E·DNA] = $0.5(K_d + E_t + D_t)^2 - [0.25(K_d + E_t + D_t)^2 - (E_tD_t)]^{1/2}$) where E_t and D_t represent enzyme and DNA concentrations, respectively.

K_d for dATP-binding and Maximum Burst Rate. Several single-nucleotide incorporation assays were performed with increasing concentrations of dATP in the nucleotide mix. Final reaction solutions contained 45 nM catalytic subunit, 256 nM accessory subunit, 250 nM 25/45-mer DNA, 50 mM Tris-HCl, pH 7.5, 100 mM NaCl, 2.5 mM $MgCl_2$, and a range of 0.2 to 8.4 μM dATP. Reactions were quenched at various times with 0.3 M EDTA. Each data set was fit with the burst equation to determine the effect of nucleotide concentration on the burst rate. The plot of these rates vs nucleotide concentration was fit to a hyperbola (burst rate = k_{pol}[dATP]/(K_d + [dATP])) to determine the K_d for dATP and the maximum rate of polymerization, k_{pol}.

Product Analysis. All polymerase assay products were separated on 15% denaturing polyacrylamide sequencing gels, imaged on a Storm 860 and quantified using ImageQuaNT software (Molecular Dynamics, Sunnyvale, CA).

RESULTS

Sequencing of cDNA and Alignment of Protein Sequences. The cDNA encoding the accessory subunit of the human mitochondrial DNA polymerase (Clone ID Number 44673) was obtained from the I. M. A. G. E. Consortium. Complete sequencing of the clone revealed an open reading frame encoding 485 amino acids. This length differs from the previously reported length of 372 amino acids (*9*) due to several deletions and one addition present in the previously published cDNA sequence, leading to a shift in the reading frame and introduction of an erroneous start codon. The corrected sequence[2] results in an additional 124 amino acids

[2] The protein sequence for the human mitochondrial DNA polymerase accessory subunit reported in this paper has been submitted to the GenBank/EMBL data bank with the accession number AAD56542.

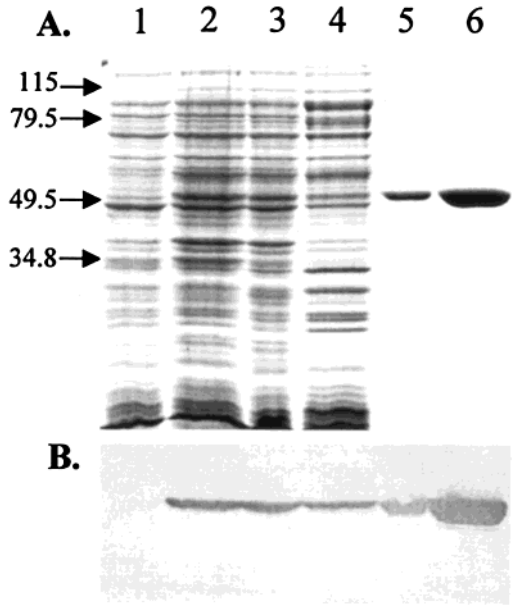

FIGURE 2: Purification of human mitochondrial DNA polymerase accessory subunit. (A) SDS-PAGE gel stained with Coomassie R-250. (B) Western blot of identical gel probed with anti 6X-histidine antibody. Lane 1: uninduced BL21(DE3) cells. Lane 2: induced BL21(DE3) cells. Lane 3: lysate of induced BL21(DE3) cells. Lane 4: soluble fraction of BL21(DE3) lysate shown in lane 3. Lane 5: fractions containing accessory subunit after chelating sepharose chromatography. Lane 6: fractions containing accessory subunit following Mono-S chromatography.

on the amino terminus of the protein, as shown in Figure 1, along with an alignment to the *Xenopus laevis* (*10*) and *Drosophila melanogaster* (*9*) amino acid sequences. The corrected open reading frame provides a new methionine start codon to give the full-length protein. To approximate the cleavage of the mitochondrial targeting signal and thereby express protein that mimics the mature, processed protein, we created a construct with a 56 amino acid truncation from the amino terminal end. This truncation site is homologous to the cleavage site in the *Xenopus* protein, which is 54% identical in sequence to the human protein. The final product has a predicted molecular mass of 49 kDa, which is only slightly smaller than the originally reported size of 54 kDa for the accessory subunit estimated by SDS-PAGE (*11*).

Bacterial Expression and Purification of Human Mitochondrial DNA Polymerase Accessory Subunit. A two-step purification was employed and is visualized in Figure 2 by SDS-PAGE and western blot analysis. A six residue histidine tag was employed for ease of protein purification. The accessory subunit[2] was purified from the soluble portion of the bacterial lysate by affinity chromatography utilizing chelating sepharose followed by cation exchange utilizing Mono-S chromatography. The resulting product has a molecular mass of 49 kDa and an estimated purity of 99% as revealed by SDS-PAGE. Protein yield was approximately 2 mg of protein from a 3 L bacterial culture.

Steady-State and Pre-Steady-State Single Nucleotide Incorporation by Mitochondrial DNA Polymerase. The steady-state rate of elongation of the 25/45-mer DNA (primer/template) to 26/45-mer product DNA by the mitochondrial DNA polymerase was measured by incubating the reconstituted holoenzyme (25 nM catalytic subunit, 140 nM accessory subunit) with a large excess of DNA (1000 nM) and

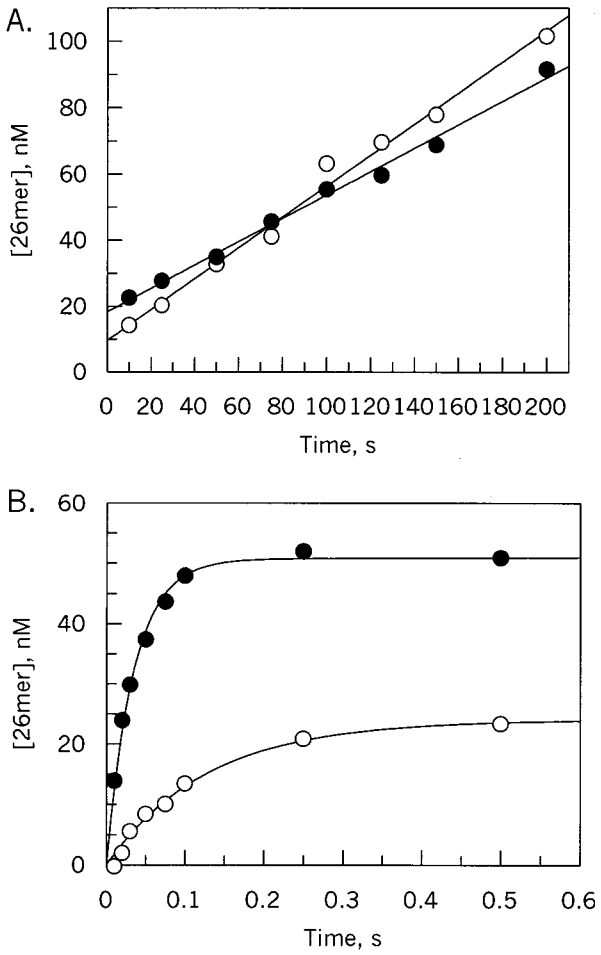

FIGURE 3: Steady-state and pre-steady-state polymerase assays. All concentrations given are final. (A) Steady-state polymerization rate. The 25 nM catalytic subunit, ±140 nM accessory subunit, was preincubated with 1 μM 25/45-mer DNA. An equal volume of a solution containing dATP (50 μM final concentration) and Mg^{2+} was added to the enzyme/DNA mix to initiate polymerization. At the time points shown, aliquots were removed and rapidly mixed with quench solution to end the reaction, and products were quantified by sequencing gel analysis as described in Experimental Procedures. The steady-state rate constant was calculated by dividing the slope of the line by the active enzyme concentration to give values for the catalytic subunit (○) and the holoenzyme (●) of 0.03 ± 0.001 s^{-1} and 0.02 ± 0.001 s^{-1}, respectively. (B) Pre-steady-state polymerization. Enzyme/DNA mix (70 nM catalytic subunit/250 nM DNA, ±400 nM accessory subunit) was rapidly combined with Mg^{2+} and dATP (250 μM), and reactions were quenched at the times indicated. Data were fit to the burst equation. The catalytic subunit (○) and holoenzyme (●) had exponential rates of 7.8 ± 0.9 s^{-1} and 29.1 ± 1.4 s^{-1} and amplitudes of 23.9 ± 1.2 and 50.7 ± 0.8 nM, respectively.

nucleotide (50 μM) substrates (Figure 3A). The slope of the line divided by the concentration of enzyme−DNA complex defines the k_{cat} of 0.02 ± 0.001 s^{-1}. This rate represents the slowest step during single nucleotide incorporation, presumably release of 26/45-mer DNA product from the enzyme. In addition, a nonzero *y*-intercept was observed indicating that a single turnover of polymerization occurred at a faster rate at earlier time points and provides an approximate measure of the concentration of enzyme-26/45-mer product formed during the first turnover. The observation of a pre-steady-state burst demonstrates that some step after chemistry is rate-limiting in the steady-state (*19*). As with all other polymerases studied in single nucleotide incorporation assays,

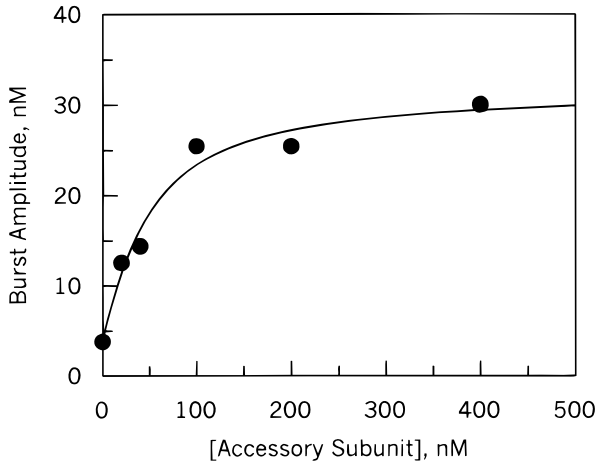

FIGURE 4: K_d for catalytic and accessory subunit interaction. All concentrations given are final. Catalytic subunit (40 nM nominal) was equilibrated with accessory subunit (0−400 nM) prior to addition of 25/45-mer DNA (200 nM). This mixture was then rapidly mixed with Mg^{2+} and dATP (50 μM) to allow formation of 26/45-mer product. Reactions were quenched at various times with 0.3 M EDTA, and products were quantified as described in Experimental Procedures. Data for each accessory subunit concentration were fit to the burst equation. The resulting burst amplitudes were plotted as a function of accessory subunit concentration and fit with a quadratic to give a K_d of 34.9 ± 16.2 nM for the protein subunits and a maximal burst amplitude of 31.8 ± 4.6 nM.

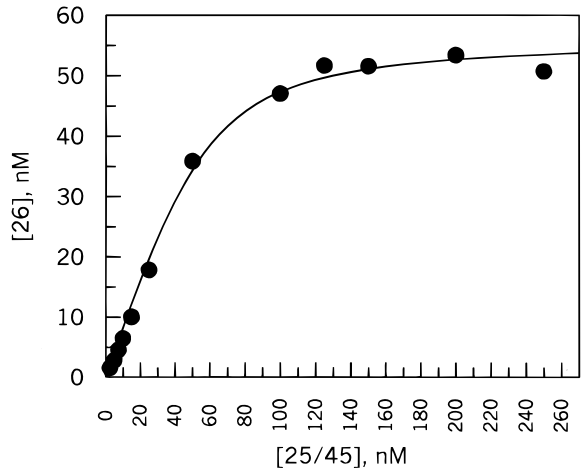

FIGURE 5: Active site titration of mitochondrial DNA polymerase. All concentrations given are final. Enzyme (70 nM nominal concentration) was preincubated with increasing concentrations of 25/45-mer DNA and then rapidly mixed with Mg^{2+} and dATP (250 μM) to initiate polymerization. Reactions were quenched after 1 s and quantified as described in Experimental Procedures. Data representing burst amplitudes at each 25/45-mer concentration were fitted to the quadratic equation to give a K_d of 9.9 ± 2.1 nM and an active enzyme concentration of 57 ± 1.5 nM.

this step is most probably release of the DNA from the enzyme and further experiments are underway to confirm this.

We examined the kinetics of the pre-steady-state single nucleotide incorporation in order to determine directly the effect of the accessory subunit on DNA polymerization catalyzed by the holoenzyme (Figure 3B). Identical experiments were performed, in the absence and the presence of the accessory subunit, at a DNA concentration approximately 4-fold higher than the concentration of the catalytic subunit. The catalytic subunit, accessory subunit, and DNA were present at concentrations of 70, 400, and 250 nM, respectively. The amount of 26-mer product was quantified, plotted against time, and fit to a burst equation ($[26mer] = A[1 - e^{-kt}] + k_{cat}t$) to obtain the burst rate and amplitude. The accessory subunit stimulated an increase in burst amplitude from 23.9 ± 1.2 to 50.7 ± 0.8 nM, indicating an increase in the concentration of productive enzyme−DNA complex that is able to form product in the first turnover. Additionally, we observed an increase from 7.8 ± 0.9 s^{-1} to 29.1 ± 1.4 s^{-1} in the fast rate of the initial incorporation of dATP, indicating faster nucleotide incorporation catalyzed by the holoenzyme.

Catalytic and Accessory Subunit Interaction. To measure the dissociation constant for the reconstitution of the holoenzyme, we titrated the catalytic subunit with increasing concentrations of the accessory subunit, measuring the effect on the amplitude of the pre-steady-state burst of single nucleotide incorporation (Figure 4). When the burst amplitudes were plotted as a function of accessory subunit concentration and fit to the quadratic equation ($[E{\cdot}DNA] = 0.5(K_d + C_t + A_t)^2 - [0.25(K_d + C_t + A_t)^2 - (C_tA_t)]^{1/2}) + B$, a maximum amplitude of 31.8 ± 4.6 nM and a K_d of 34.9 ± 16.1 nM for the dimer formation were obtained. The data are consistent with a stoichiometry of 1:1 in the final complex in that the saturation curve approaches limiting asymptotes for a 1:1 complex, not a 1:2 complex. We are in the process of analyzing the stoichiometry by methods that more directly measure the ratio of proteins in the complex.

Active Site Titration. To determine the dissociation constant for DNA-binding to the holoenzyme and the concentration of active enzyme, we titrated the holoenzyme with increasing concentrations of DNA and measured the pre-steady-state burst amplitude in single nucleotide incorporation assays. This assay provides an estimate of the concentration of productive E·DNA complexes, because incorporation is much faster than DNA dissociation and rebinding. The burst amplitudes were plotted as a function of DNA concentration and the data were fit to the quadratic equation ($[E{\cdot}D] = 0.5(K_d + E_t + D_t)^2 - [0.25(K_d + E_t + D_t)^2 - (E_tD_t)]^{1/2}$). As shown in Figure 5, the K_d for the reconstituted mitochondrial DNA polymerase holoenzyme was 9.9 ± 2.1 nM. This value is 3.5-fold tighter than that seen in the absence of the accessory protein (*8*). The active enzyme concentration was 57 ± 1.5 nM, indicating 82% of the catalytic subunit is active relative to calculated concentrations based upon absorbance measurements.

Nucleotide Dissociation Constant and Maximum Polymerization Rate. The kinetic parameters governing nucleotide incorporation were determined by examining the nucleotide concentration dependence of the burst rate. The preequilibrated polymerase−DNA complex (formed with saturating accessory protein and DNA) was combined with various concentrations of dATP and the rate of the pre-steady-state burst of polymerization was measured. The rates were plotted as a function of dATP concentration (Figure 6) and fit to a hyperbola (burst rate $= k_{pol}[dATP]/(K_d + [dATP])$). A K_d of 0.78 ± 0.065 nM for nucleotide ground-state binding and a maximum rate, k_{pol} of 45 ± 1 s^{-1} were obtained.

DISCUSSION

We have reconstituted a human mitochondrial DNA polymerase holoenzyme consisting of recombinantly expressed and purified catalytic and accessory subunits. We

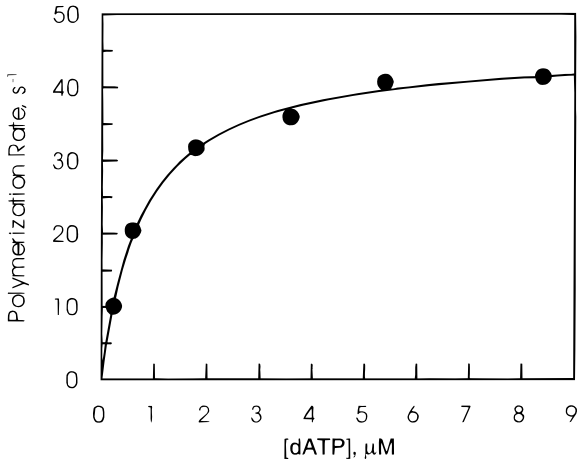

FIGURE 6: K_d for nucleotide and determination of maximum burst rate. All concentrations given are final. Enzyme (70 nM nominal concentration) was preincubated with 25/45-mer DNA (250 μM) and then rapidly mixed with Mg^{2+} and increasing concentrations of dATP (0.2−8.4 μM). The burst rates obtained for each dATP concentration were plotted as a function of dATP concentration. Fit of the data to a hyperbola to yield a K_d for dATP of 0.78 ± 0.065 μM and a maximum polymerization rate of 45 ± 1 s^{-1}.

Table 1. Kinetic Parameters of the Mitochondrial DNA Polymerase Catalytic Subunit and Holoenzyme

	catalytic subunit	holoenzyme
k_{pol}	8.7 ± 1.1 s^{-1}	45 ± 1 s^{-1}
K_d, DNA	39 ± 10 nM[a]	9.9 ± 2.1 nM
K_d, dATP	4.7 ± 2.0 μM	0.78 ± 0.065 μM
k_{off}	0.03 ± 0.001 s^{-1}	0.02 ± 0.001 s^{-1}
processivity[b]	290 ± 46	2250 ± 162

[a] Value for K_d for DNA-binding by the catalytic subunit was taken from (*8*). [b] Processivity was calculated as $k_{pol}/k_{off.}$

previously investigated the basic characteristics of the polymerase and 3′−5′ exonuclease activities that reside in the human catalytic subunit (*8*). Here we demonstrate that the accessory subunit plays a role in tighter polymerase-binding to the DNA and to the nucleotide and an increased rate of nucleotide incorporation into DNA. A comparison of kinetic parameters exhibited by the holoenzyme and those of the catalytic subunit is provided in Table 1.

The steady-state rate of polymerization by the mitochondrial DNA polymerase holoenzyme was determined to be 0.02 ± 0.001 s^{-1} (Figure 3A). The steady-state rate is determined by the slowest step during polymerization, which must occur after the chemical reaction to account for the observation of a pre-steady-state burst. In a single nucleotide incorporation experiment, the rate-limiting step is presumably the dissociation of the enzyme from DNA. This rate was only slightly slower than the rate of 0.03 ± 0.001 s^{-1} observed in the absence of the accessory protein. Given the 4-fold effect of the accessory protein on the K_d for DNA-binding, these data suggest that the accessory protein increases the rate of DNA-binding without greatly affecting the dissociation rate.

The dissociation constant for the two-subunit complex was 35 ± 16 nM. The stoichiometry of the complex has not been determined and further experiments are underway to address this question, although the titration data (Figure 4) are most consistent with the formation of a 1:1 complex with a K_d of 35 ± 16 nM. A K_d of 5 nM was observed between T7 DNA polymerase and thioredoxin (*20*), suggesting the interaction observed between the DNA polymerase γ subunits is reasonable. Additionally, native γ polymerase purified from *Drosophila* and human tissues exhibit a molecular ratio of 1:1 following sedimentation and gel filtration analyses (*9*, *11*). Although the K_d of 35 nM for binding the accessory protein is reasonably tight, this interaction may be weak enough that the accessory subunit is lost from the complex during purification of the native enzyme from tissue (*9*). This would account for the variable activity seen in preparations of protein from native tissues. In our current experiments, we have employed a molar ratio of approximately 1:6 (catalytic subunit to accessory subunit) in order saturate the binding to attain a maximum rate of polymerization as well as maximal enzyme association with 25/45-mer DNA. Most experiments on T7 DNA polymerase have employed a 20-fold molar excess of thioredoxin accessory protein (*22*).

The K_d for DNA-binding to the holoenzyme was 9.9 ± 2.1 nM. In the presence of the accessory subunit, the interaction between the DNA and the polymerase is approximately 4-fold stronger than that observed between DNA and the catalytic subunit alone. Thioredoxin exerts a similar effect on T7 DNA polymerase where the binding affinity is increased 20−30-fold in the presence of the accessory subunit (*21*). Additionally, the DNA-binding affinity of the mitochondrial DNA polymerase holoenzyme is very similar to that of other polymerases studied (*18*, *22*, *23*). The presence of the accessory subunit probably allows the DNA-binding site to be in a position that can more tightly grasp the DNA by enhancing interactions between the DNA and the catalytic subunit. However, the most profound affects of the accessory protein are on nucleotide-binding and incorporation.

Both the K_d for nucleotide ground-state binding and the rate of nucleotide incorporation by the mitochondrial DNA polymerase are significantly enhanced by the presence of the accessory subunit. The dissociation constant for dATP-binding by the catalytic subunit and the holoenzyme were 3.9 ± 1.6 and 0.78 ± 0.065 μM, respectively. The value for holoenzyme-binding is somewhat lower than the K_d for correct nucleotide observed for other polymerases, which is typically 5−20 (*18*, *22*, *23*). In our assays, nucleotide and magnesium are introduced to a tightly bound, preformed enzyme−DNA complex to allow polymerization to occur. Incorporation occurs at a maximal rate of 45 ± 1 s^{-1}, a significant increase over the rate of 8.7 ± 1.1 s^{-1} exhibited by the catalytic subunit alone.

It seems logical that the accessory protein may contribute structural stability to the catalytic subunit allowing it to bind nucleotide more tightly and to catalyze faster polymerization. The nucleotide may bind to the holoenzyme more tightly, because the active site is in a conformation that is closer to the state required for catalysis. Following nucleotide-binding, most polymerases undergo a conformational change to position the substrates for catalysis (*19*). An increase in the burst rate indicates the holoenzyme undergoes a faster conformational change or faster chemical reaction, which is facilitated by the binding of the accessory subunit. Thus, we propose that the accessory protein must contribute to and alter the structure of the catalytic subunit. The rate of DNA release is minimally affected, probably due to similar DNA-binding site conformations following polymerization, and the binding of the DNA through electrostatic interactions over a large area of the surface of the polymerase (*24*).

Another well-characterized accessory protein, thioredoxin, functioning with T7 DNA polymerase, shows much more profound effects on the DNA-binding affinity and affords a significant decrease in the DNA dissociation rate (*21*). Crystal structures have shown that thioredoxin is attached to the flexible thumb domain of T7 DNA polymerase. Thioredoxin extends this thumb domain, and it is suggested that thioredoxin moves to form a lid enclosing the DNA within the binding pocket to obviate DNA release and increase processivity (*24*). This interaction may lead to the decrease in the rate of DNA dissociation by T7 DNA polymerase in association with thioredoxin. Similar DNA dissociation rates from the catalytic subunit and holoenzyme of DNA polymerase γ suggest the accessory subunit is not acting to physically keep product DNA bound to the polymerase. The active sites must be in the same or very similar positions within both the catalytic subunit and the holoenzyme for the chemical reaction to occur, leading to similar rates of DNA dissociation.

Polymerase accessory proteins are often described as processivity factors or clamps. However, it is important to remember that processivity is a ratio of at least two kinetic constants and that anything that improves polymerization or DNA-binding will be reflected in an increased processivity. Carrodegaus et al. (*10*), has shown increased extension of singly primed M13 single-stranded DNA and poly(dA)-oligo(dT) DNA by the mitochondrial DNA polymerase in the presence of the accessory subunit using a hybrid heterodimer composed of the human catalytic subunit and the *Xenopus* accessory subunit. Williams et al. (*25*) showed that less pure fractions of *Drosophila* DNA polymerase γ exhibited greater extension of singly primed M13 single-stranded DNA, possibly indicating loss of an accessory factor during purification that would increase processivity. We calculated a processivity value for the mitochondrial DNA polymerase of 2250 by dividing k_{pol} by k_{off}, which is approximately 8-fold lower in the absence of the accessory protein. But, it is significant that the increase in calculated processivity results almost entirely from an increase in the rate of polymerization. In comparison, the presence of thioredoxin leads to a significant decrease in the dissociation rate of the enzyme−DNA complex as well as an increase in the polymerization rate (*26*, Patel, S. S., and Johnson, K. A., unpublished data). Together, these data show that the accessory subunit allows highly processive replication of the mitochondrial DNA by increasing the forward polymerization rate. Given a mitochondrial genome of 16 kb in length, a forward polymerization rate of 45 s^{-1} would allow one polymerase heterodimer to replicate one copy of the genome in less than six minutes, in eight binding events.

The accessory subunit of human DNA polymerase γ appears to play an essential role in the interaction of the enzyme with substrates to facilitate efficient replication, allowing faster polymerization and tighter substrate-binding. Determining the kinetic parameters governing polymerization efficiency exhibited by this enzyme may provide a baseline for screening of nucleoside analogues. For example, in vivo evidence of inhibition of replication by DNA polymerase γ in the presence of nucleoside analogues suggests incorrect nucleotides are bound with higher affinity by the mitochondrial DNA polymerase or removed less efficiently by the proofreading exonuclease compared to other cellular polymerases (*27*). A thorough examination of the nucleotide incorporation mechanism, and the efficiency of the 3′−5′ exonuclease will be essential to understanding the fidelity of the mitochondrial DNA polymerase and its relationship to in vivo observations of nucleoside analogue toxicity. Additional articles addressing mitochondrial DNA polymerase holoenzyme formation have been published recently (*28*, *29*).

ACKNOWLEDGMENT

We would like to thank Dr. Kevin Dalby and members of his laboratory for assistance during preparation of this manuscript.

REFERENCES

1. Wallace, D. C. (1992) *Science 256*, 628−632.
2. Naviaux, R. K., Nyhan, W. L., Barshop, B. A., Poulton, J., Markusic, D., Karpinski, N. C., and Haas, R. H. (1999) *Ann. Neurol. 45*, 54−8.
3. Parker, W. B., and Cheng, Y. C. (1994) *J. NIH Res. 6*, 57−61.
4. Nusbaum, N. J., and Joseph, P. E. (1996) *DNA Cell Biol. 15*, 363−366.
5. Wernette, C. M., and Kaguni, L. S. (1986) *J. Biol. Chem. 261*, 14764−14770.
6. Insdorf, N. F., and Bogenhagen, D. F. (1989) *J. Biol. Chem. 264*, 21419−21497.
7. Olson, M. W., and Kaguni, L. S. (1992) *J. Biol. Chem. 267*, 23136−23142.
8. Graves, S. W., Johnson, A. A., and Johnson, K. A. (1998) *Biochemistry 37*, 6050−6058.
9. Wang, Y, Farr, C. L., and Kaguni, L. S. (1997) *J. Biol. Chem. 272*, 13640−13646.
10. Carrodeguas, J. A., Kobayashi, R., Lim, S. E., Copeland, W. C., and Bogenhagen, D. F. (1999) *Mol. Cell. Biol. 19*, 4039−4046.
11. Gray, H., and Wong, T. W. (1992) *J. Biol. Chem. 267*, 5835−5841.
12. Mosbaugh, D. W. (1988) *Nucleic Acids Res. 16*, 5645.
13. Ropp, P. A., and Copeland, W. C. (1996) *Genomics 36*, 449−458.
14. Lecrenier, N., Van Der Bruggen, P., and Foury, F. (1997) *Gene 185*, 147−152.
15. Lewis, D. L., Farr, C. L., Wang, Y., Lagina, A. T., and Kaguni, L. S. (1996) *J. Biol. Chem. 271*, 23389−23394.
16. Longley, M. J., Ropp, P. A., Lim, S. E., and Copeland, W. C. (1998) *Biochemistry 37*, 10529−10539.
17. Pace, C. N., Vajdos, F., Fee, L., Grimsley, G., and Gray, T. (1995) *Protein Sci. 4*, 2411−2423.
18. Kati, W. M., Johnson, K. A., Jerva, L. F., and Anderson, K. S. (1992) *J. Biol. Chem. 267*, 25988−25997.
19. Johnson, K. A. (1992) *Philos. Trans. R. Soc. London, Ser. B. 336*, 107−112.
20. Huber, H. E., Russel, M., Model, P., and Richardson, C. C. (1986) *J. Biol. Chem. 261*, 15006−15012.
21. Huber, H. E., Tabor, S., and Richardson, C. C. (1987) *J. Biol. Chem. 262*, 16224−16232.
22. Patel, S. S., Wong, I., and Johnson, K. A. (1991) *Biochemistry 30*, 511−525.
23. Kuchta, R. D., Mizrahi, V., Benkovic, P. A., Johnson, K. A., and Benkovic, S. J. (1987) *Biochemistry 26*, 8410−8417.
24. Doublie, S., Tabor, S., Long, A. M., Richardson, C. C., and Ellenberger, T. (1998) *Nature 391*, 251−258.
25. Williams, A. J., Wernette, C. M., and Kaguni, L. S. (1993) *J. Biol. Chem. 269*, 24855−24862.
26. Tabor, S., Huber, H. E., and Richardson, C. C. (1987) *J. Biol. Chem. 262*, 16212−16223.
27. Starnes, M. C., and Cheng, Y.-C. (1987) *J. Biol. Chem. 262*, 988−991.
28. Wang, Y., and Kaguni, L. S. (1999) *J. Biol. Chem. 274*, 28972−28977.
29. Lim, S. Ee., Longley, M. J., and Copeland, W. C. (1999) *J. Biol. Chem. 274*, 38197−38203.

BI992104W